

Modeling and Simulation of Orientation-Dependent Fluctuations in Nanowire Field-Effect Biosensors using the Stochastic Linearized Poisson-Boltzmann Equation

Clemens Heitzinger and
Norbert J. Mauser
Department of Mathematics &
Wolfgang Pauli Institute
University of Vienna
Vienna, Austria
Email: Clemens.Heitzinger@univie.ac.at,
Mauser@courant.nyu.edu

Christian Ringhofer
Department of Mathematics
Arizona State University
Tempe, Arizona
Email: Ringhofer@asu.edu

Yang Liu and
Robert W. Dutton
Center for Integrated Systems
Stanford University
Palo Alto, California
Email: yangliu@gloworm.stanford.edu,
rdutton@stanford.edu

Abstract—We use the stochastic linearized Poisson-Boltzmann equation to model the fluctuations in nanowire field-effect biosensors due to changes in the orientation of the biomolecules. Different orientations of the biomolecules with respect to the sensor surface due to Brownian motion have different probabilities. The probabilities of the orientations are calculated from their electrostatic free energy. The structure considered here is a cross section through a rectangular silicon nanowire lying on an oxide surface with a back-gate contact. The oxide surface of the nanowire is functionalized by biomolecules in an electrolyte with an electrode. Various combinations of PNA (peptide nucleic acid), single-stranded DNA, and double-stranded DNA are simulated to discuss the various states of a DNA sensor. A charge-transport models yields the current through the transducer that compares well with measurements.

I. INTRODUCTION

Affinity-based field-effect nano-biosensors have been demonstrated experimentally [1]–[3]. Their working principle is that the oxide surface of a silicon nanowire is functionalized by receptor molecules. As analyte molecules bind to the receptors at the surface in an aqueous solution, the analyte molecules change the charge concentration in the biofunctionalized boundary layer (see Fig. 1). This, in turn, results in a change of the conductance of the nanowire transducer that can be measured. The sensors are selective, since only matching molecules can bind to the receptor molecules at the surface. The sensors are sensitive, since the amount of conductance change yields quantitative information about the biomolecules at the surface. The main advantage of this technology is label-free operation, whereas currently employed technology works by labeling the analyte molecules.

Despite recent advances in their theoretic understanding [4]–[7], many questions about the physics of the sensors remain open.

In this work we introduce a PDE-based model for fluctuations or noise in these biosensors; more precisely, we use a stochastic PDE for the electric potential in biosensors. The model can also be applied to similar structures and to other sources of noise. Our aim is to investigate how the stochastic charge concentrations in the boundary layer influence the current through the transducer.

In actual biosensors, the charge concentration at the transducer surface is a probability distribution, i.e., it depends on a random variable. The randomness is due to binding and unbinding events of analyte molecules depending on the binding efficiency of receptor and target molecules and it is due to changes in the orientation of the biomolecules with respect to the surface (Brownian motion).

II. THE STOCHASTIC LINEARIZED POISSON-BOLTZMANN EQUATION

The model for the electric potential ϕ in the biosensor used here is the stochastic linearized Poisson-Boltzmann equation

$$L\phi(x, \omega) = \rho(x, \omega), \quad (1)$$

where ω is a random variable, $\phi(x, \omega)$ is the electric potential, and L is the linear differential operator

$$L := -\nabla \cdot (A(x)\nabla) + \gamma(x),$$

where $A(x)$ is the permittivity. The right-hand side

$$\rho(x, \omega) := \rho_f(x, \omega) + \alpha(x)$$

includes the fixed charge concentration $\rho_f(x, \omega)$. The terms $\alpha(x)$ and $\gamma(x)$ on the right-hand sides stem from linearization. This most general form of the Poisson-Boltzmann equation is derived from a Boltzmann distribution with Fermi level ϕ_F for

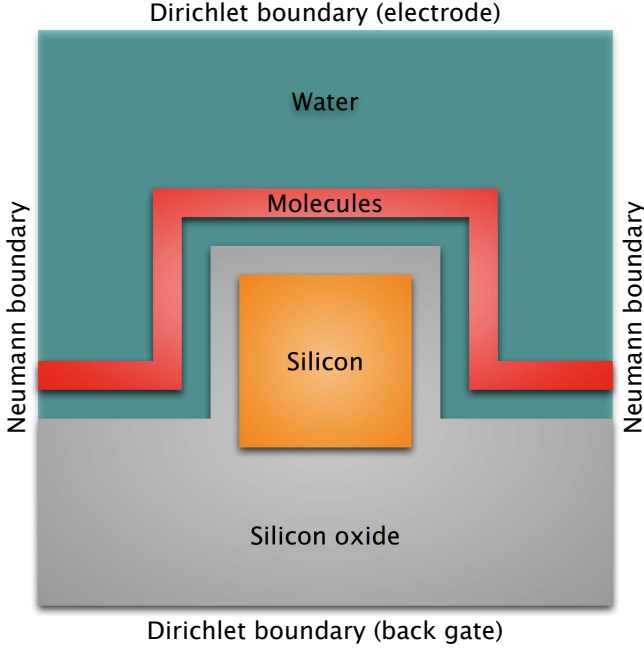


Fig. 1. Schematic diagram of the cross section of the nanowire field-effect biosensor considered in this work.

the mobile charges in the electrolyte in the Poisson equation and linearization by Taylor expansion around ϕ_0 . This gives

$$\begin{aligned}\alpha(x) &:= 2c(x)q \sinh \frac{q(\phi_F - \phi_0)}{k_B T} \\ &\quad + \frac{2c(x)q^2 \phi_0}{k_B T} \cosh \frac{q(\phi_F - \phi_0)}{k_B T}, \\ \gamma(x) &:= \frac{2c(x)q^2}{k_B T} \cosh \frac{q(\phi_F - \phi_0)}{k_B T},\end{aligned}$$

where $c(x)$ is the bulk concentration of the ions, q is the elementary charge, k_B is the Boltzmann constant, and T is the temperature.

To understand the fluctuations of the electric potential and therefore the noise arising from the random charge concentration, it is necessary to calculate its expectation $E\phi$ and its variance $\sigma^2\phi$. The expectation is treated more easily than the variance. Since the linear operator L and the expectation operator E commute at least formally, i.e.,

$$EL\phi(x, \omega) = LE\phi(x, \omega),$$

the expectation $E\phi$ is the solution of the equation

$$LE\phi(x, \omega) = E\rho(x, \omega).$$

This equation has the same form as (1).

To simplify the analysis, we define the shifted charge concentration $\tilde{\rho}$ and the shifted potential $\tilde{\phi}$ as

$$\begin{aligned}\tilde{\rho} &:= \rho - E\rho, \\ \tilde{\phi} &:= \phi - E\phi,\end{aligned}$$

so that $E\tilde{\rho} = 0$, $E\tilde{\phi} = 0$, and

$$L\tilde{\phi} = \tilde{\rho}$$

hold.

A simple calculation using the definition of the variance shows that

$$\sigma^2\phi = \sigma^2\tilde{\phi}$$

holds for the variance of the potential and of the shifted potential.

III. RESULTS FROM HOMOGENIZATION AND A SCALING LAW

A question that arises naturally is: how does the size of the fluctuations scale with the size of the biomolecules? Do smaller biomolecules in the functionalized boundary layer result in less fluctuations and by how much? To answer this question, we now summarize a result leading to a scaling law for the variance and covariance. The proofs and the details will be published elsewhere.

The physical situation we consider is a three-dimensional nanowire sensor structure. The boundary layer at the oxide surface is partitioned into boxes that contain different charge concentrations representing different molecules and different orientations. The coordinate system is locally so that x_1 is normal to the surface and x_2 and x_3 are parallel to the surface. For each cell k , there is a random variable ω_k and its different states can correspond to different molecules and different orientations and combinations thereof. The random variable ω is defined by

$$\omega := (\omega_1, \dots, \omega_K),$$

the charge concentration of cell k is denoted by $\rho_k(x, \omega_k)$, and we write the cumulative charge concentration as

$$\rho(x, \omega) = \sum_k \chi_k(x) \rho_k(x, \omega_k),$$

where $\chi_k(x)$ is the characteristic function of cell k .

The main result is the following. Here ϵ is the zoom factor between slow and fast variables, i.e., it is the ratio between the size of a box and the whole domain.

Theorem. *The covariance $\text{cov}(\tilde{\phi})$ is the solution of the equation*

$$\begin{aligned}L_\xi L_x \text{cov}(\tilde{\phi})(x, \xi) &= \epsilon^4 \delta(x_1, \xi_1, \xi_2 - x_2, \xi_3 - x_3) \cdot \\ &\quad \cdot \int_{\Omega(x_2, x_3)} R(\omega(x_2, x_3))^2 d\omega(x_2, x_3),\end{aligned}$$

where

$$R(\omega_k) := \int_0^\infty \int_0^1 \int_0^1 \tilde{\rho}(y_1, y_2, y_3, \omega_k) dy_3 dy_2 dy_1.$$

Here L_ξ and L_x are the differential operator L with respect to the ξ and x variables, respectively.

This homogenization result immediately yields this corollary.

Corollary. The covariance $\text{cov}(\tilde{\phi})$ and the variance scale as ϵ^4 for $\epsilon \rightarrow 0$.

This result answers the question posed above. Since ϵ is the spatial ratio between the size of (a box containing) a molecule to the size of the whole simulation domain, it means that smaller molecules yield much reduced variance or fluctuations: the variance reduces even as ϵ^4 . This means that smaller molecules can be detected much more efficiently than larger ones regarding noise due to Brownian motion.

IV. SIMULATION RESULTS

We present simulation results for the nanowire DNA sensor whose structure is shown in Fig. 1. We consider different combinations of PNA (peptide nucleic acid) and DNA strands in the boundary layer. PNA is an uncharged molecule similar to DNA and it is often used in the functionalization of sensor surfaces, since PNA and DNA bind very well. In the situations in Table I, one strand is always the receptor strand and the second strand is the analyte strand.

Depending on the orientation of the DNA strands with respect to the surface, the thickness of the molecule layer (red) is calculated from the double-helix structure of B-DNA and the same known total charge is distributed uniformly in each case according to a simple analytical model.

We rotate axes of the PNA and DNA strands with respect to the surface and consider these different charge concentrations. The probabilities of the different orientations of ssDNA and dsDNA are calculated from their electrostatic free energy as in [8]. Then the orientation i with the electrostatic free energy E_i is assigned the probability

$$p_i := \frac{\exp(-E_i/(k_B T))}{\sum_i \exp(-E_i/(k_B T))}$$

according to a Boltzmann distribution.

Next, we calculate the expectation $E\phi$ and variance $\sigma^2\phi$ (which immediately gives the standard deviation $\sigma\phi$) of the electric potential in a cross section. A simulation result is shown in Fig. 2 and Fig. 3. It is observed that the standard deviation has local maxima at the corners of the molecule layer. The variance and the standard deviation vanish at the bulk-gate and electrode contacts due to the Dirichlet boundary conditions used there. Neumann boundary conditions are used at the rest of the boundaries.

Finally, we calculate the currents $I(E\phi)$ and $I(E\phi \pm \sigma\phi)$. Since $\sigma\phi \ll 1$, this is a good approximation of the expected current and its standard deviation. Using the known potential values $\phi(x, y)$ in the cross section, the current through the transducer is calculated as

$$I(\phi) = n_i q \mu_p F \int \exp\left(\frac{q\phi_F - q\phi(x, y)}{k_B T}\right) dx dy - n_i q \mu_n F \int \exp\left(\frac{-q\phi_F + q\phi(x, y)}{k_B T}\right) dx dy,$$

where n_i is the intrinsic carrier density of the nanowire, μ_p and μ_n are the carrier mobilities, and $F = 50\text{mV}/1\mu\text{m}$ is the electric field in longitudinal direction.

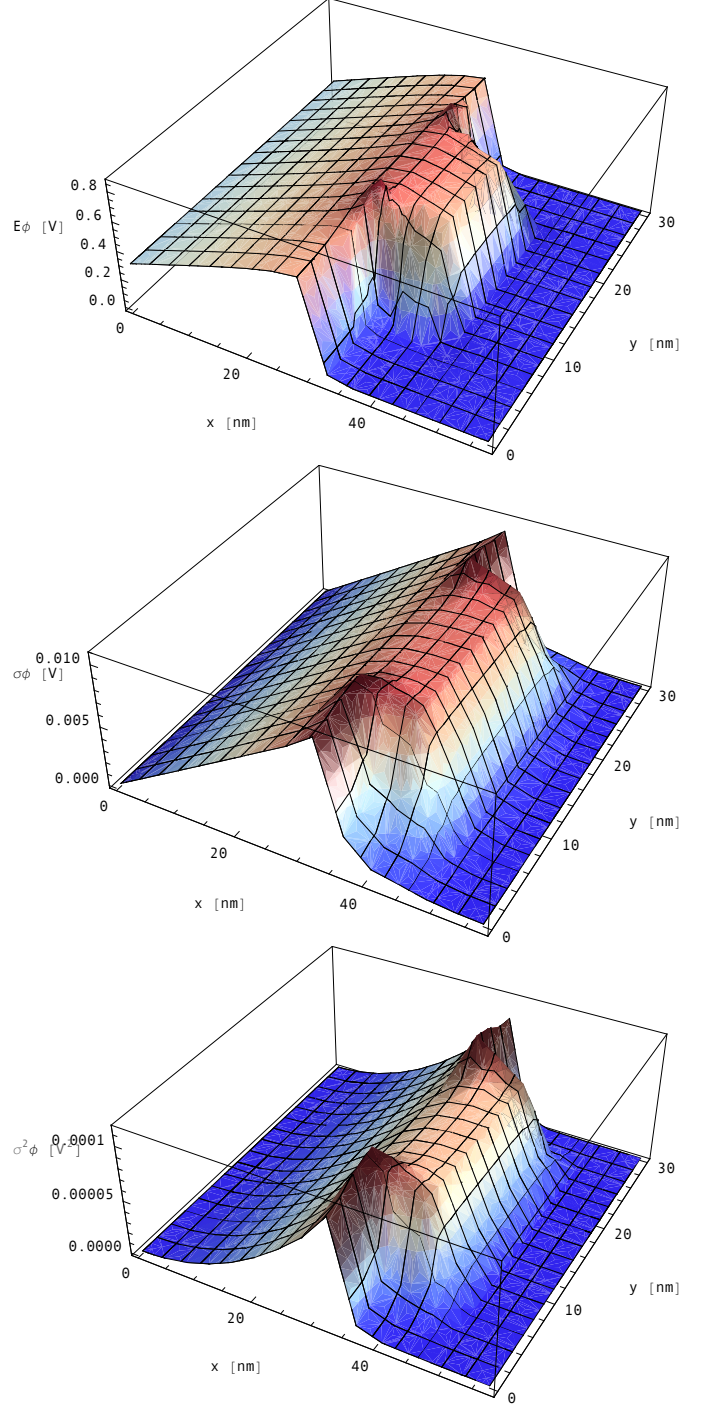


Fig. 2. Expectation $E\phi$ (top), standard deviation $\sigma\phi$ (middle), and variance $\sigma^2\phi$ (bottom) of the electric potential in the cross section of the structure corresponding to the third row in Table I, i.e., the one with the largest variance. The x -axis is normal to the oxide substrate and the y -axis is parallel to the substrate. There are 30nm of oxide substrate, the nanowire has a cross section of $10\text{nm} \cdot 10\text{nm}$, its doping concentration is $10^{18} \text{q}/\text{cm}^3$, its Fermi level is 0.3V, the oxide thickness is 2nm, the surface charge density is $0.2\text{q}/\text{nm}^2$, the molecules are located at 0.5nm from the oxide surface, and the Na^+Cl^- concentration is 30mM.

TABLE I
SIMULATION RESULTS FOR VARIOUS MOLECULES, FOR VARIOUS SPACINGS BETWEEN THE MOLECULES, AND FOR VARIOUS BINDING EFFICIENCIES BETWEEN RECEPTOR AND TARGET MOLECULES.

Receptor spacing	Molecules	Current	Change
5nm	50% PNA & 50% ssDNA	$I(E\phi - \sigma\phi) = -2.498 \cdot 10^{-8} \text{ A}$	-26.78%
		$I(E\phi) = -3.412 \cdot 10^{-8} \text{ A}$	0 %
		$I(E\phi + \sigma\phi) = -4.659 \cdot 10^{-8} \text{ A}$	+36.58%
5nm	100% ssDNA	$I(E\phi - \sigma\phi) = -2.311 \cdot 10^{-8} \text{ A}$	-8.020%
		$I(E\phi) = -2.512 \cdot 10^{-8} \text{ A}$	0 %
		$I(E\phi + \sigma\phi) = -2.731 \cdot 10^{-8} \text{ A}$	+8.719%
5nm	50% ssDNA & 50% dsDNA	$I(E\phi - \sigma\phi) = -1.275 \cdot 10^{-8} \text{ A}$	-29.27%
		$I(E\phi) = -1.803 \cdot 10^{-8} \text{ A}$	0 %
		$I(E\phi + \sigma\phi) = -2.549 \cdot 10^{-8} \text{ A}$	+41.38%
5nm	100% dsDNA	$I(E\phi - \sigma\phi) = -1.156 \cdot 10^{-8} \text{ A}$	-10.67%
		$I(E\phi) = -1.294 \cdot 10^{-8} \text{ A}$	0 %
		$I(E\phi + \sigma\phi) = -1.449 \cdot 10^{-8} \text{ A}$	+11.95%
10nm	100% ssDNA	$I(E\phi - \sigma\phi) = -3.893 \cdot 10^{-8} \text{ A}$	-2.068%
		$I(E\phi) = -3.976 \cdot 10^{-8} \text{ A}$	0 %
		$I(E\phi + \sigma\phi) = -4.060 \cdot 10^{-8} \text{ A}$	+2.112%
10nm	100% dsDNA	$I(E\phi - \sigma\phi) = -3.274 \cdot 10^{-8} \text{ A}$	-2.782%
		$I(E\phi) = -3.368 \cdot 10^{-8} \text{ A}$	0 %
		$I(E\phi + \sigma\phi) = -3.464 \cdot 10^{-8} \text{ A}$	+2.862%

Table I collects simulation results for different boundary layers where 12-mers of PNA (uncharged), single-stranded DNA (ssDNA), and double-stranded DNA (dsDNA) are present with different probabilities due to different molecule concentrations in the liquid. The first two rows are the results for ssDNA detection by PNA receptors. In the first row, 50% of the receptors are bound to ssDNA strands that are detected. In the second row, 100% of the receptors are bound to ssDNA strands. These numbers show that a higher binding

efficiency of target ssDNA to receptor PNA decreases noise significantly. Put differently, if the concentration of analyte or target molecules in the liquid and thus at the sensor surface is higher, the noise is less.

In the third row, ssDNA strands are detected by ssDNA receptors and 50% of the receptors are bound to target strands. In the fourth row, 100% of the receptors are bound. The third and fourth row show again that noise is less at the 100% binding efficiency level compared to the 50% level. Compared to the first and second row, there is slightly more noise when ssDNA receptors are used for ssDNA detection (third and fourth row) than when PNA receptors are used (first and second row).

In the last two rows, the spacing between the molecules was increased from 5nm to 10nm. Here we compare the current for 100% ssDNA in the fifth row to the current for 100% dsDNA in the sixth row. A comparison between the second and the fifth row and a comparison between the fourth and the sixth row shows that the noise level is reduced by approximately a factor of 4 as expected.

V. CONCLUSION

We have developed a PDE-model based on the stochastic linearized Poisson-Boltzmann equation to calculate fluctuations in nanowire field-effect biosensors. The model can also be applied to fluctuations due to stochastic effects in charge concentrations in similar structures as well.

This model makes it possible to calculate the expectation and standard deviation of the electric potential and of the cur-

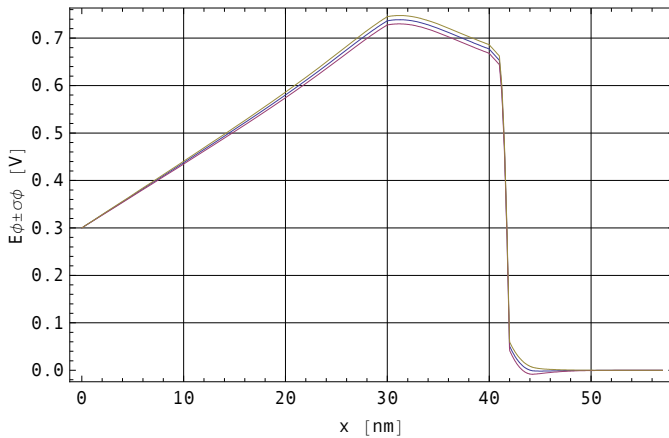


Fig. 3. Expectation $E\phi$ (middle curve) and expectation plus/minus standard deviation $E\phi \pm \sigma\phi$ (top and bottom curves) of the electric potential corresponding to Fig. 2 through the middle of the structure at $y = 15\text{nm}$.

rent in the transducer depending on the probability distribution of the charge concentration in the functionalized boundary layer where molecular recognition takes place in affinity-based sensors.

The computational approach is efficient since it is based on a linear stochastic PDE. If a Monte Carlo procedure were used, many more solutions of the Poisson equation would have to be calculated to just estimate the expectation and variance. Further computational improvements in the calculation of the variance and covariance, i.e., in the most time-consuming part, enable the simulation of larger structures and will be presented elsewhere.

The simulation results and the published experimental values are in good agreement. Finally, we also discussed a scaling law for the variance and covariance as the size of the molecules in the boundary layer goes to zero.

VI. ACKNOWLEDGMENT

This work was supported by the ÖAW (Austrian Academy of Sciences) jubilee-fund project *Multi-Scale Modeling and Simulation of Field-Effect Nano-Biosensors* and the FWF (Austrian Science Fund) project P20871-N13 *Mathematical Models and Characterization of BioFETs*.

REFERENCES

- [1] J. Hahn and C. M. Lieber, "Direct ultrasensitive electrical detection of DNA and DNA sequence variations using nanowire nanosensors," *Nano Lett.*, vol. 4, no. 1, pp. 51–54, 2004.
- [2] Y. Bunimovich, Y. Shin, W.-S. Yeo, M. Amori, G. Kwong, and J. Heath, "Quantitative real-time measurements of DNA hybridization with alkylated nonoxidized silicon nanowires in electrolyte solution," *J. Amer. Chem. Soc.*, vol. 128, p. 16323–16331, 2006.
- [3] E. Stern, J. Klemic, D. Routenberg, P. Wyrembak, D. Turner-Evans, A. Hamilton, D. LaVan, T. Fahmy, and M. Reed, "Label-free immunodetection with CMOS-compatible semiconducting nanowires," *Nature*, vol. 445, pp. 519–522, Feb. 2007.
- [4] C. Heitzinger, R. Kennell, G. Klimeck, N. Mauser, M. McLennan, and C. Ringhofer, "Modeling and simulation of field-effect biosensors (BioFETs) and their deployment on the nanoHUB," *J. Phys.: Conf. Ser.*, vol. 107, pp. 012004/1–12, 2008. [Online]. Available: <http://www.iop.org/EJ/abstract/1742-6596/107/1/012004>
- [5] C. Ringhofer and C. Heitzinger, "Multi-scale modeling and simulation of field-effect biosensors," *ECS Transactions*, vol. 14, no. 1, pp. 11–19, 2008.
- [6] Y. Liu, K. Lilja, C. Heitzinger, and R. W. Dutton, "Overcoming the screening-induced performance limits of nanowire biosensors: a simulation study on the effect of electro-diffusion flow," in *IEDM 2008 Technical Digest*, San Francisco, CA, USA, Dec. 2008, pp. 491–494.
- [7] A. Bulyha, C. Heitzinger, and N. Mauser, "Three-dimensional Monte Carlo simulation of biofunctionalized surface layers in the constant-voltage ensemble," *SIAM J. Sci. Comput.*, *Submitted for publication*.
- [8] A. H. Talasaz, M. Nemat-Gorgani, Y. Liu, P. Ståhl, R. W. Dutton, M. Ronaghi, and R. W. Davis, "Prediction of protein orientation upon immobilization on biological and nonbiological surfaces," *Proc. Nat. Acad. Sci. U.S.A.*, vol. 103, no. 40, pp. 14773–14778, Oct. 2006.